JOURNAL OF MAGNETIC RESONANCE **126,** 30–38 (1997)
ARTICLE NO. MN971144

Shielding of Low-Frequency Magnetic Interference in Weak-Field MRI by a Single-Layer Cylindrical Coil

Gorazd Planinšič

Physics Department, University of Ljubljana, Jadranska 19, 1000 Ljubljana, Slovenia

Received July 22, 1996; revised February 10, 1997

Shielding of detection coil from low-frequency magnetic-field interference is one of the main problems in weak-field MRI methods that utilize cycling of main magnetic field (MRI in the Earth's magnetic field, for example). In such cases, the best solution is usually to shield the detection coil by shorting one of the resistive coils of the system, typically the magnetization coil. The optimization of this shielding method has been done by studying the total magnetic field on the axis of a shorted single-layer cylindrical coil placed in a homogeneous oscillating magnetic field parallel to the coil axis. The results are generalized for the case when series impedance is added to the shielding coil. The optimal added impedance that gives the largest shielding factor in the center of the coil is calculated. Because the theoretical treatment is confined to the coil axis, the results are in simple form ready to use in applications. The results of the calculation are verified experimentally and implemented in Earth's field MRI system.

INTRODUCTION

MR imaging in weak magnetic fields, ranging from 0.5 G (Earth's magnetic field) up to few 100 G, is gaining increased attention during the past years. Most weak-field MRI methods utilize switching of the static magnetic field (field cycling) either to prepolarize the sample in a relatively strong magnetic field (*1–3*) or to decrease the RF power deposition during saturation of electron transitions in dynamic-nuclear-polarization-enhanced MRI (*4, 5*).

Our homemade Earth's-magnetic-field imaging system performs a field cycling experiment (*6*). The water sample is magnetized in a magnetic field of 500 G. Then the magnetization field is adiabatically switched off, leaving the sample magnetization pointing in the direction of the residual Earth's magnetic field. After a 90° pulse, the sample magnetization is flipped into the plane perpendicular to the Earth's field direction, where a free-induction signal with a frequency around 2 kHz can be observed. At such low frequency, copper screens do not efficiently suppress magnetic interference from the environment unless very thick copper or mu-metal plates are used. However, cycling the magnetic field inside the metal cage produces eddy currents in the cage walls, which causes an additional decaying inhomogeneous magnetic field which destroys the NMR signal. For this reason, shielding of the detection coil from low-frequency magnetic-field interference is one of the main problems in very-weak-field MRI. One possible solution of this problem is to choose one of the resistive coils (usually magnetization coil) which is parallel to detection coil axis and shorts it during signal detection. In this case, the magnetic-field interference inside the coil is partially shielded by the currents that this same interference induces in the shorted coil. Though this approach is well known in weak-field MRI (*1–3, 5, 7*), the full description and optimization of shielding the oscillating magnetic field by the coil has not been described before, to the author's knowledge.

THEORY

In practice, it can be assumed that magnetic interference is caused by a distant source. In this case, the interference at the site of the coil can be treated as a plane wave of magnetic field.

Let the single-layer coil with shorted terminals be placed in the external homogeneous oscillating magnetic field $B = B_0 e^{i\omega t}$ parallel to the coil axis. The induced current in the coil creates an additional magnetic field which opposes the external magnetic field. In the following treatment, the resultant (shielded) magnetic field on the coil axes is analyzed. It is assumed that the frequency of field oscillation is much smaller than self-resonant frequency of the solenoid and that the distributed capacitance of the coil can be neglected.

The schematic circuit of the shorted coil is shown in Fig. 1, where U_i is the induced voltage in the coil, L is the inductance, and R is the resistance of the coil. The induced current in the circuit can be calculated using Kirchoff 's law

$$IR + L\frac{dI}{dt} = U_i\,. \qquad [1]$$

The induced voltage in the coil is then given by

$$U_i = -\frac{d\Phi}{dt} = -iN\pi a^2\omega B_0 e^{i\omega t} \qquad [2]$$

1090-7807/97 $25.00

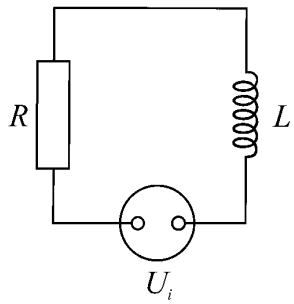

FIG. 1. Equivalent circuit for a shorted coil.

and the induced current from Eq. [1] by

$$I_i = -\frac{U_0}{\sqrt{R^2 + (L\omega)^2}}\, e^{i(\pi/2-\varphi)}, \qquad [3]$$

where U_0 is amplitude of induced voltage and

$$\varphi = \arctan\frac{\omega L}{R} = \arctan Q. \qquad [4]$$

The magnetic field due to the induced current in the solenoid can be expressed in the form

$$B_s = \frac{\mu_0 N I_i}{l}\, f(z', r), \qquad [5]$$

where l is the length of the solenoid and $f(r, z')$ is the function describing the geometry of the magnetic field of a solenoid alone. The function $f(r, z')$ can be calculated using the Biot–Savart law. In practice, we are mainly interested in the field near the coil axes inside the solenoid. Therefore, we shall use the expression for $f(r = 0, |z'| \leqslant l/2)$ which has a simple analytical form

$$f(z) = \frac{1}{2}\left[\frac{1 - z}{\sqrt{(1 - z)^2 + \beta^2}} + \frac{1 + z}{\sqrt{(1 + z)^2 + \beta^2}}\right], \qquad [6]$$

where $\beta = 2a/l$ and coordinate z is measured in half lengths of the solenoid

$$z = \frac{2z'}{l}.$$

The origin of coordinate system is placed at the center of the coil with the z axis parallel to the coil axis. The induced current creates a magnetic field $\mathbf{B}_s$ which adds to the external magnetic field $\mathbf{B}$. On the coil axis, $\mathbf{B}_s$ is parallel to $\mathbf{B}$. From Eqs. [2], [3], [5], the total magnetic field can be expressed in the form

$$B_{\text{tot}} = B_0(1 - qe^{i(\pi/2-\varphi)})e^{i\omega t}, \qquad [7]$$

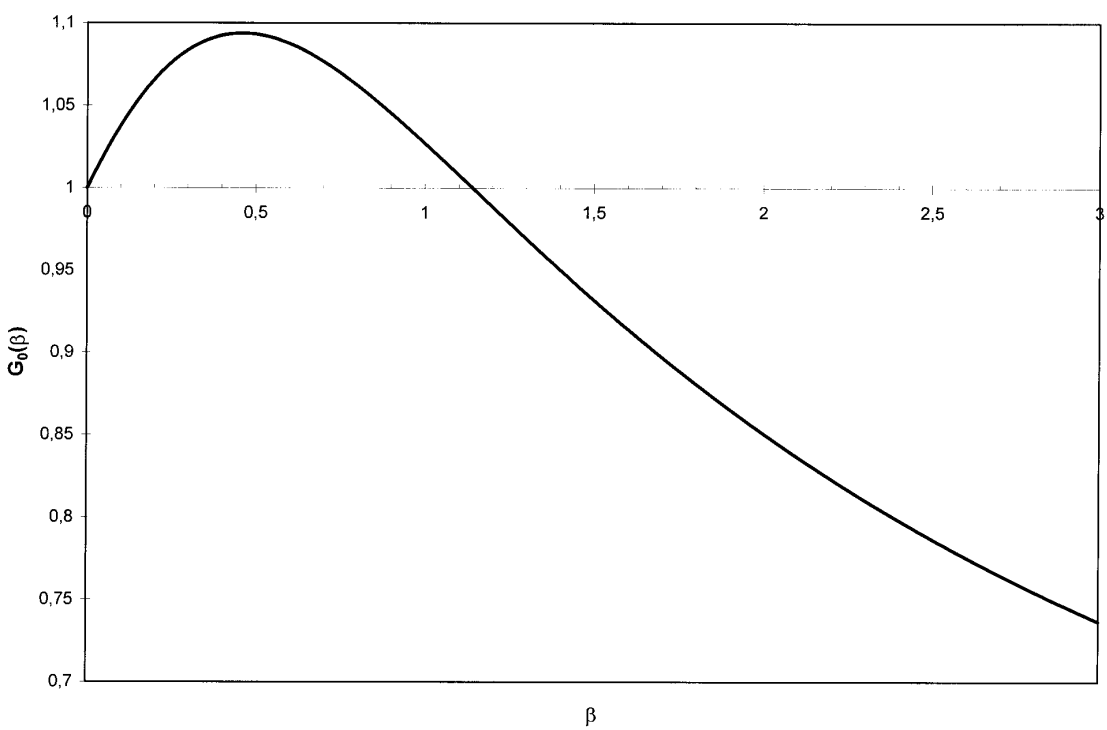

FIG. 2. Dependence of function $G_0(\beta)$ on coil geometry factor $\beta = 2a/l$.

where

$$q = \mu_0 \frac{N^2 \pi a^2 \omega}{l\sqrt{R^2 + (\omega L)^2}} f(z). \quad [8]$$

The self-inductance of the single-layer cylindrical coil is given by the expression

$$L_s = \frac{\mu_0 N^2 \pi a^2}{l} \eta(\beta), \quad [9]$$

where η is function of ratio β. Function $\eta(\beta)$ is given by the expression (*8*)

$$\eta(\beta) = \frac{4}{3\pi\beta}\left[\frac{K(k^2) + (\beta^2 - 1)E(k^2)}{k} - \beta^2\right], \quad [10]$$

where

$$k^2 = \frac{\beta^2}{1 + \beta^2}$$

and K and E are complete elliptical integrals of the first and second kind. In practice, the function $\eta(\beta)$ is usually replaced by a long-coil or short-coil approximation. It will be clear later that the exact expression for $\eta(\beta)$ should be used in order to optimize the shielding characteristics of the coil. Using Eqs. [8] and [9], we write q in a compact form

$$q = \frac{G(z, \beta)}{\sqrt{1 + Q^{-2}}}, \quad [11]$$

where

$$G(z, \beta) = \frac{f(z)}{\eta(\beta)}.$$

Using Eq. [7], the shielding factor of the coil F can be expressed as

$$F = \frac{|B_{tot}|}{B_0} = \sqrt{1 + q^2 - 2q \sin\varphi}, \quad [12]$$

and the phase angle of B_{tot} with respect to B in the form

$$\theta = \arccos\frac{1 + F^2 - q^2}{2F}. \quad [13]$$

It can be seen from Eq. [4] that phase angle φ approaches 0 in the small-Q limit ($Q \ll 1$) and $\pi/2$ in the high-Q limit ($Q \gg 1$). Therefore, in the high-Q limit, the shielding magnetic field B_s opposes the external field B—the coil works as a low-pass filter.

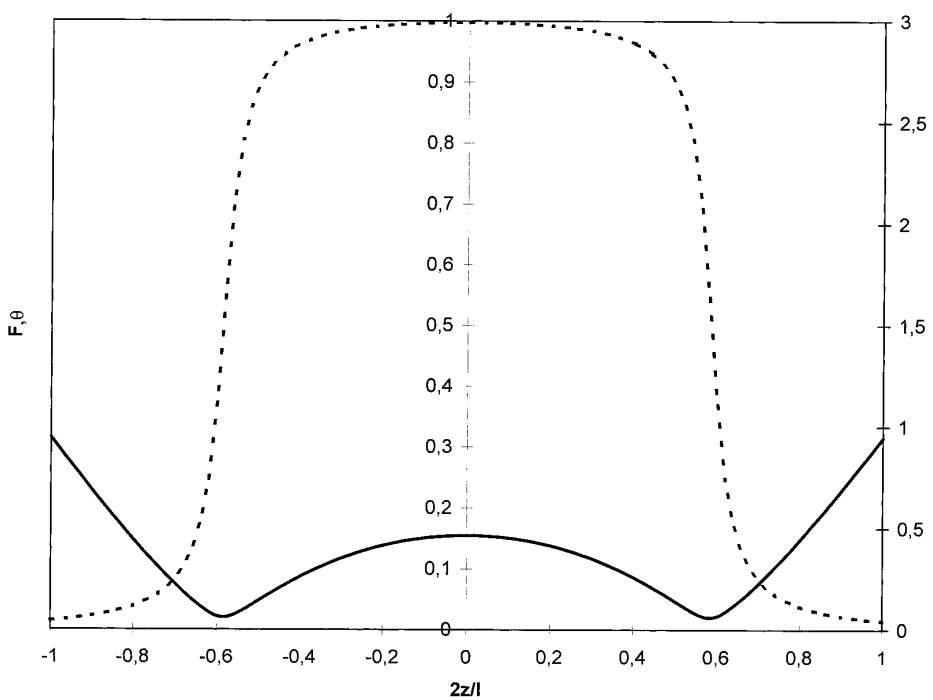

FIG. 3. The dependence of shielding factor F (solid line) and phase angle θ (broken line) on the position along the coil axes ($Q = 50$, $\beta = 0.8$). The phase-angle values are measured in radians and displayed on the secondary vertical axis.

Equations [11] and [12] suggest that the dependence of shielding characteristics of the coil on its geometry is described by the function $G(z, \beta)$. In the center of the coil, we get

$$G_0(\beta) = G(0, \beta) = \frac{1}{\eta(\beta)\sqrt{1 + \beta^2}}. \qquad [14]$$

The graph of $G_0(\beta)$ is shown in Fig. 2. It can be concluded from the graph and from Eqs. [11] and [12] that the coil with $\beta \approx 0.46$ will produce the largest shielding field in its center. Since in this case $G_0(\beta) \approx 1.094 > 1$, it can be expected that the shielding field in the center of the coil can even exceed the external magnetic field (which produced it), providing that Q of the coil is high enough. Because the shielding field decreases to zero from the coil center, there should exist two points on the coil axes where B_{tot} reaches the minimum value. The example of calculation of shielding factor and the phase angle θ along the axes of a long coil (Eqs. [12], [13]) is shown in Fig. 3.

It can be shown that for the coils with large Q the shielding factor F has an approximate value

$$F \approx \sqrt{(1 - G)^2 + (2 - G)G\,\frac{1}{Q^2}}, \qquad [15]$$

where $G = G(z, \beta)$. In the center of the coil, Eq. [15] reaches a minimum value of $1/Q$ for $G_0(\beta) = 1$ which corresponds to $\beta \approx 1.14$. In other words, the coil with $\beta \approx 1.14$ will produce the best shielding in its center. Any other geometry of the coil will shield its center less efficiently. Note that even in very high frequency limit, when the term with Q^{-2} in Eq. [15] can be neglected, the total field at the coil center is still different from zero, unless $G_0(\beta) = 1$!

From now on, we shall use the term ''long coil'' for coils with $G_0(\beta) > 1$ and ''short coil'' when $G_0(\beta) < 1$. For short coils, the shielding field in the center of shorted coil cannot exceed the external field. The minimum of B_{tot} is always in the center of the short coil, but shielding is less efficient than for the long coil.

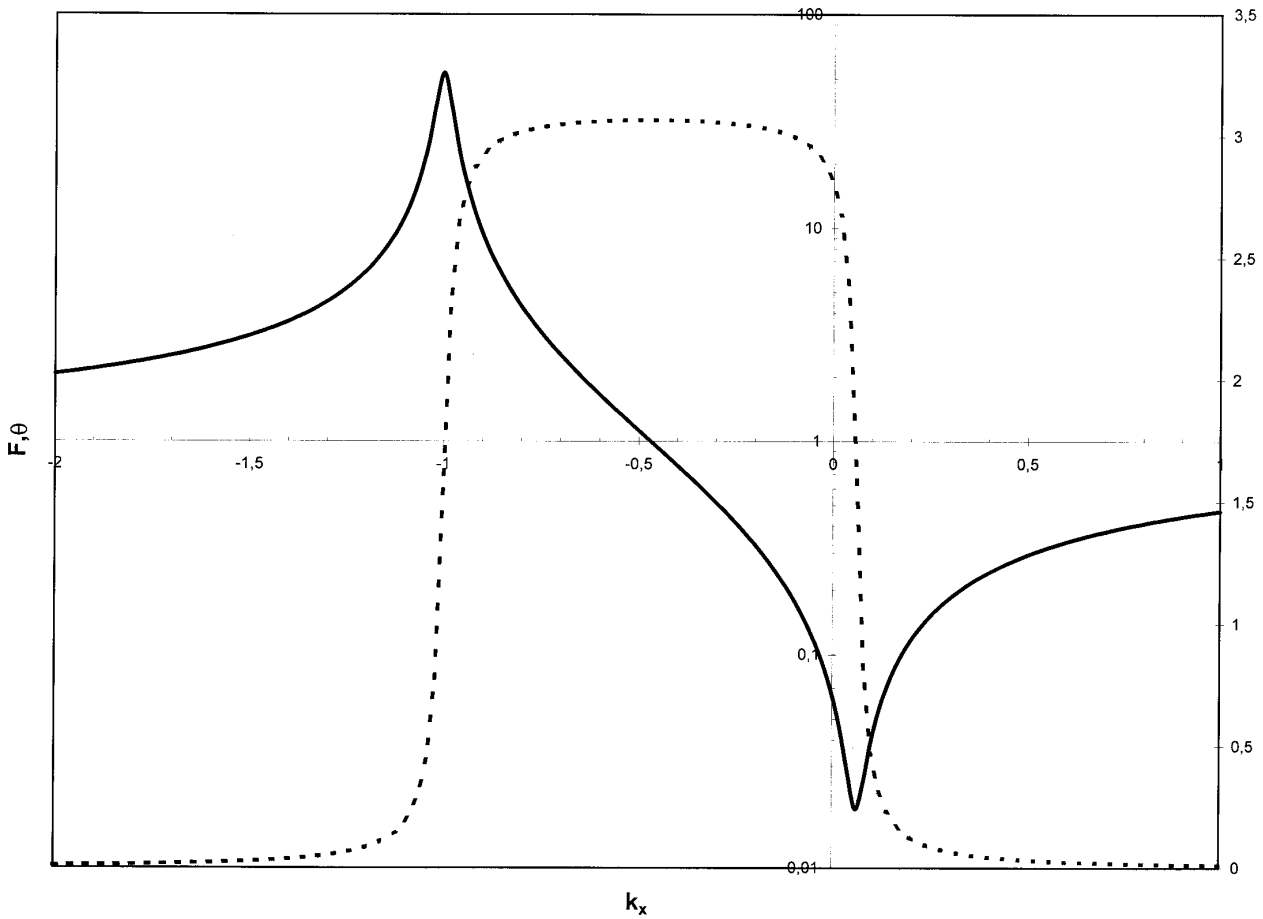

FIG. 4. The dependence of shielding factor F (solid line) and phase angle θ (broken line) in the center of the coil on the added series reactance X_s ($k_x = X_s/i\omega L$). The coil parameters are $Q = 50$, $\beta = 0.8$, and $k_r = 0$. The shielding factor is displayed on a logarithmic scale, and phase values are measured in radians and displayed on the secondary axes.

TABLE 1
Measured Parameters of the Coils Used in the Experiment and for MRI in the Earth's Magnetic Field (HP 4284-A LCR Meter)

Coil	1 (mm)	2r (mm)	d_w (mm)	N	R_{DC} (Ω)	L (μH)	Q_{1kHz}	Q_{15kHz}
Coil A	100	77	1.9	28	0.04	33.7	5	44
Coil B	33	83	1.9	16	0.03	23.9	6	39
Max. pair (one loop)	20	460	0.65	200	6.5	8890	—	—
Pick-up coil	6	12	0.5	12	≈0.04	18.4	—	—
Earth's field magnetization coil	684	397	4 × 6	640	≈0.5	70000	—	—
Earth's field detection coil	110	110	0.2	6000	520	2.57	≈10	—

Obviously, the long shielding coil which produces the total magnetic field as shown in Fig. 3 does not work as a good shield in the region near the coil center—the region where NMR detection coils are normally placed. It would be therefore very useful if the two minimums in Fig. 3 could be moved to the center of the coil. This can be done by altering the shielding field (i.e., altering the induced current) of the coil. Since coil impedance can be increased or decreased by adding inductor or capacitor in series to the coil, the value of B_s will increase/decrease as well, providing the induced voltage was constant. The induced voltage will remain constant if the added inductor or capacitor is well isolated from the external magnetic field so that it does not affect the total induced voltage in the circuit. This is almost always true for capacitors but not for inductors. The inductors should be screened or wound on toroidal forms in order to minimize the interaction between external magnetic field and inductor.

The shielding characteristics of the coil with the added isolated impedance (reactance X_s and resistance R_s) in series can be derived by using the results from the previous paragraph. If the total impedance is written as

$$Z = (R + R_s) + i(\omega L + X_s),$$

then the expressions for parameter q and phase angle φ (Eqs. [4], [11]) can be written in the form

$$q = \frac{G(z, \beta)}{\sqrt{(1 + k_x)^2 + Q'^{-2}}}, \qquad [16]$$

$$\varphi = \arctan(Q'(1 + k_x)), \qquad [17]$$

where

$$k_x = \frac{X_s}{\omega L}, \qquad [18]$$

$$k_r = \frac{R_s}{R}, \qquad [19]$$

$$Q' = \frac{Q}{1 + k_r}. \qquad [20]$$

Negative k_x value corresponds to the added series capacitance

$$C_s = \frac{1}{\omega^2 L |k_x|}; \qquad [21]$$

positive k_x values correspond to added series inductance

$$L_s = k_x L. \qquad [22]$$

In case of the added capacitance, the added resistance is almost negligible ($k_r \approx 0$), while in case of added inductance it may be substantial. The effect of added impedance on shielding factor F and phase angle θ in the center of the coil is shown on the example of a long coil with $Q = 50$ and $\beta = 0.8$ (see the graph in Fig. 4).

It can be concluded from Fig. 4 that the shielding performance of this particular coil can be optimized by terminating the coil with the series inductance $L_s \approx 0.06L$. The improvement in shielding factor, compared to the shielding factor of a shorted coil ($k_x = 0$), is more than threefold. For clarity, the added resistance R_s was neglected in this calculation. Ratio k_r is always positive and it appears only in Eq. [20]. Therefore in most practical cases, the added resistance ''spoils'' a small fraction of the shielding factor but it does not change the shape of the $F(k_x)$ dependence significantly.

The $F(k_x)$ and $\theta(k_x)$ values in the center of an arbitrary coil have dependence very similar to that shown in Fig. 4 (providing that Q of the coil is not too low), except that the minimum in $F(k_x)$ appears at different k_x values. For short coils, the minimum appears at negative k_x (added series capacitance) and for long coils at positive k_x values (added series inductance). Using Eqs. [16] and [17] in Eq. [12], the shielding factor in the coil with added series impedance can be expressed as a function of parameter k_x. From the first derivative, the minimum of this function is found to be at

$$k_x^{op} = \frac{G}{2}\left(1 + \sqrt{1 + \frac{4}{G^2 Q'^2}}\right) - 1 \qquad [23]$$

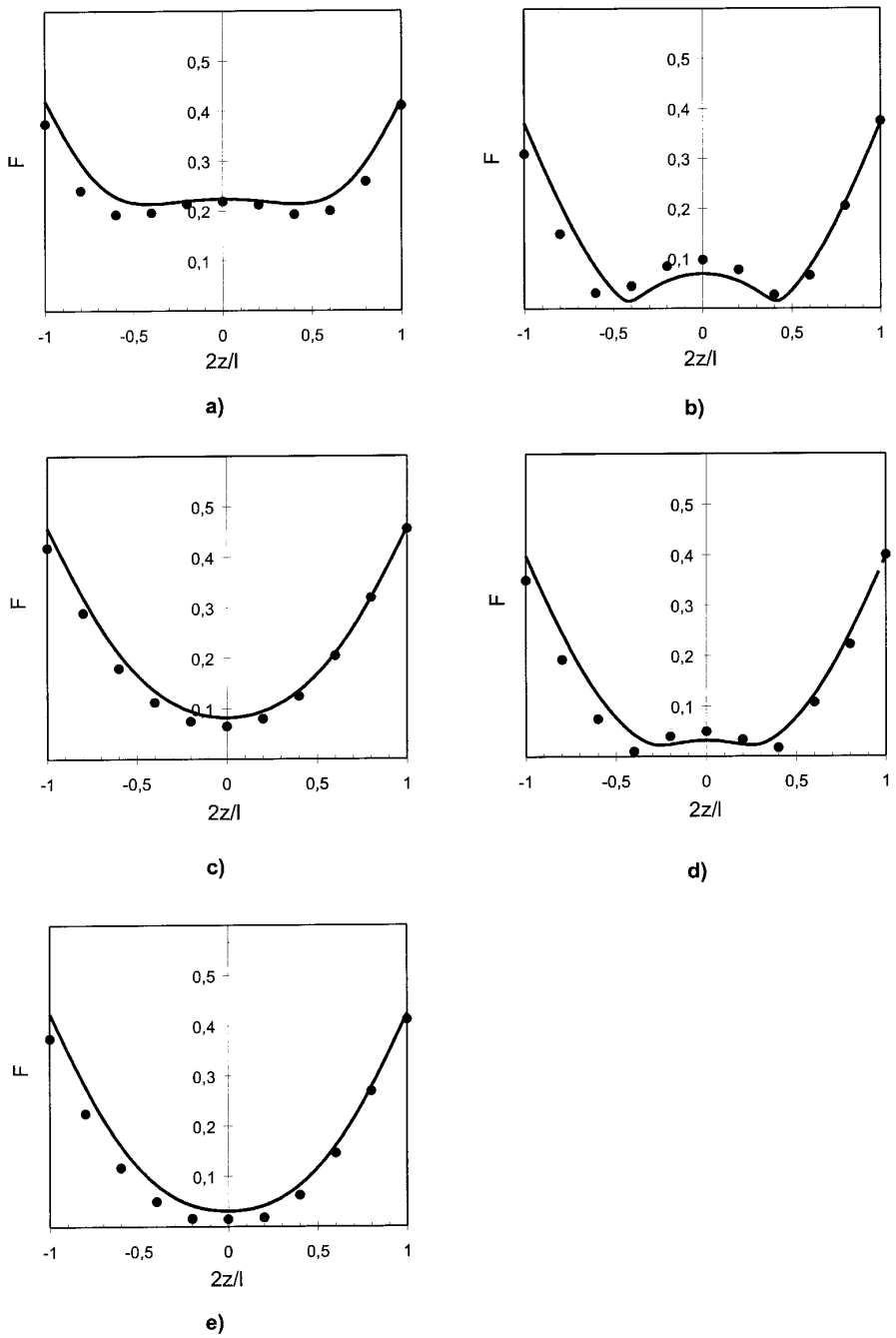

FIG. 5. Measured (points) and calculated (lines) shielding factor along the axis of the shorted coil *A* (see Table 1) at external magnetic-field frequency of (a) 1 kHz and (b) 15 kHz. Measured and calculated shielding factors at 15 kHz for long coil with added series inductance with $k_r \approx 0.6$ and (c) $k_x = 0.16$, (d) $k_x = 0.044$, and (e) $k_x = 0.092$ (see Eqs. [18], [19]). The calculated optimal series inductance in this case is $k_x^{opt} = 0.068$ (obtained from Eq. [23] at an average measured value of $k_r = 0.6$).

with the corresponding shielding factor and its high Q limit

$$F^{op} = \sqrt{\frac{\sqrt{1 + \frac{4}{G^2 Q'^2}} - 1}{\sqrt{1 + \frac{4}{G^2 Q'^2}} + 1}} \approx \frac{1}{GQ'}, \qquad [24]$$

where $G = G(z, \beta)$.

The maximum of $F(k_x)$ always appears at $k_x \approx -1$ when the circuit is in resonance with the external field frequency. It can be shown that the separation between the minimum and maximum is inversely proportional to $G(\beta)$. This must be considered when shielding with added capacitance is performed. Obviously, it is desired that minimum (best shielding) is as far as possible from resonant point. On the other hand, when inductance is used to optimize the

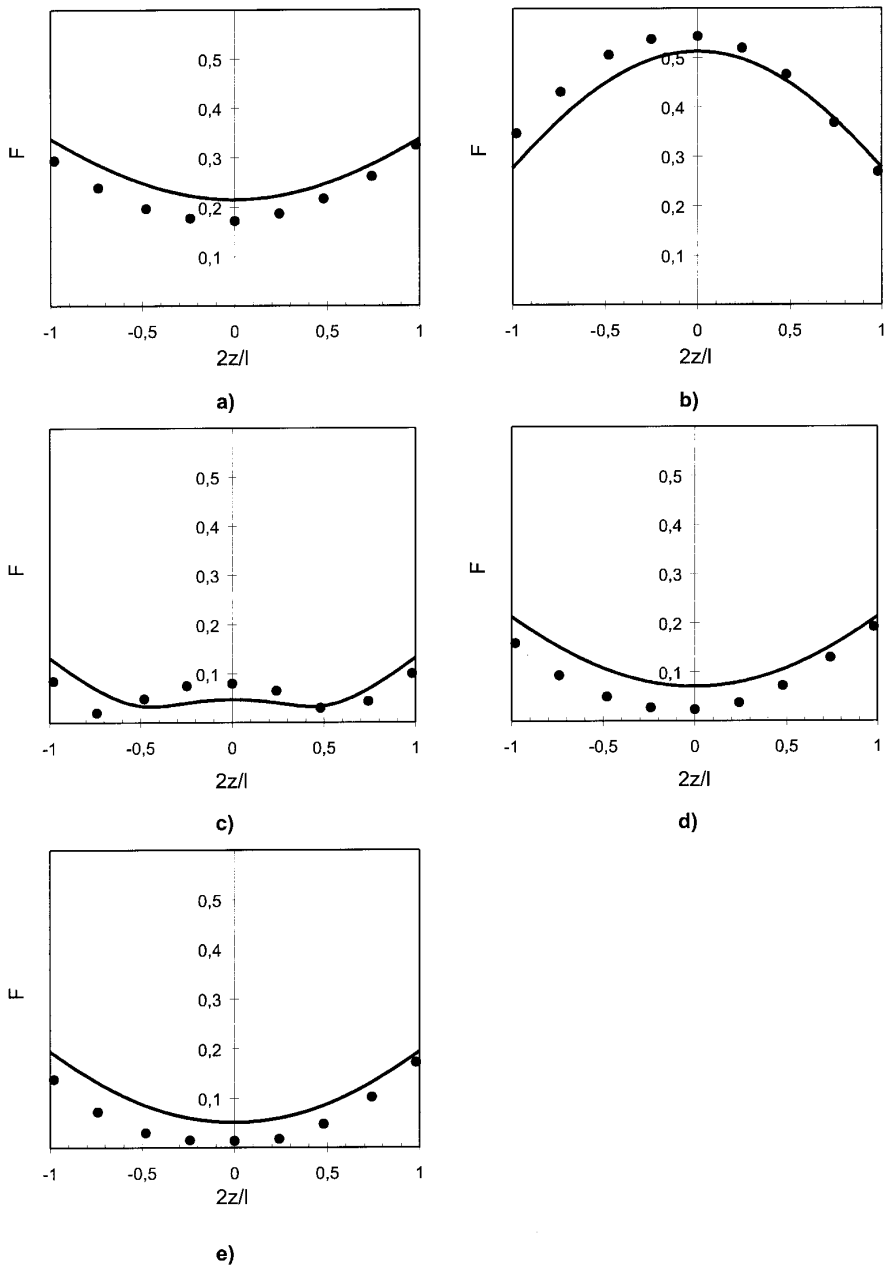

FIG. 6. Measured (points) and calculated (lines) shielding factors along the axis of coil B (see Table 1) at external magnetic-field frequency of 15 kHz with (a) shorted coil terminals and with added series capacitance with (b) $k_x = -0.48$, (c) $k_x = -0.24$, (d) $k_x = -0.16$, and (e) $k_x = -0.18$ (see Eq. [18]). The calculated optimal series capacitance in this case is $k_x^{\mathrm{opt}} = -0.21$ (obtained from Eq. [23] for $k_r = 0$).

shielding, the frequency characteristics of the circuit do not change much from those of the shorted coil. The circuit behaves as a low-pass filter with no resonant points as long as the frequency is well below the self-resonance frequency of the coil.

EXPERIMENT

The theory developed in the previous section was experimentally verified on the bench using a common laboratory equipment. The oscillating magnetic field was generated with the Maxwell pair connected to an audio amplifier and to a signal generator. The shielding coil (coil under observation) was placed in the center of the Maxwell pair. The two coils of the Maxwell pair were driven in parallel in order to minimize mutual inductance between the shielding coil and the Maxwell pair. The magnetic-field amplitude was measured inductively with a small pick-up coil. The signal was amplified and observed on the oscilloscope. First, the magnetic field on the axis of the Maxwell pair was measured.

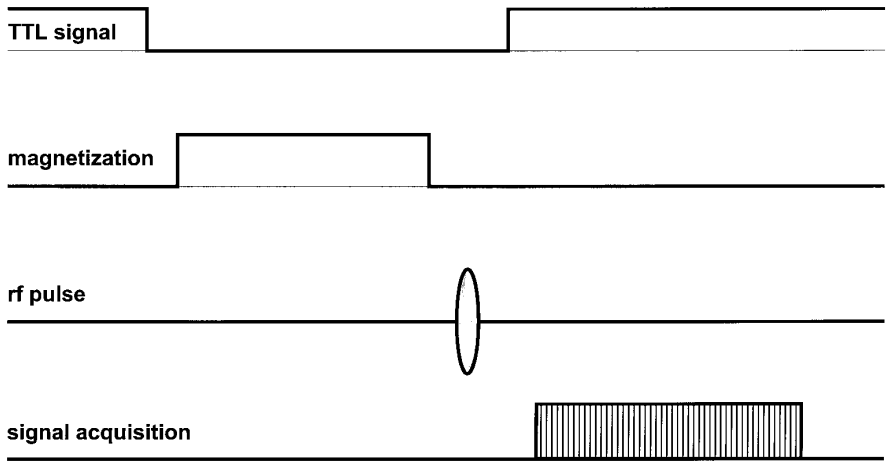

FIG. 7. The pulse sequence for observing an FID in the Earth's magnetic field. The TTL signal closes the switch and shorts the magnetization coil with the added optimal impedance (1 = shorted coil).

Then the shielding coil was inserted and the magnetic field along the axis of shielding coil was measured. Finally, the shielding factor at each point on the axes was calculated as a ratio between the two amplitudes. The measured values of coil parameters are given in Table 1.

The comparison between measured and calculated values of the shielding factor for shorted coils at frequencies 1 and 15 kHz has been done on different coils. In all cases, the theoretical and measured values were in good agreement despite the assumptions made in the model (the homogeneous oscillating magnetic field and neglected distributed capacitance of the coil windings), the positioning error, and the finite size of the pick-up coil. Some results are shown in Figs. 5 and 6.

The effect of added series impedance on the shielding factor was also examined. The comparison between measured and calculated shielding factors along the long-coil axis for different added inductance is shown in Fig. 5. The same comparison for a short coil with different added capacitance is shown in Fig. 6. Again, the calculated and measured optimal added impedance factors k_x^{op} are in good agreement.

Using the theory described above, the S/N ratio of our homemade Earth's-magnetic-field MR imaging system (see the Introduction) was improved. The external interference was shielded only by shorting the magnetization coil with optimal added impedance during signal detection. Shorting of the coil was performed by a relay controlled by a TTL signal from the computer. The example for a simple pulse sequence is shown in Fig. 7. Note that the relay shorts the magnetization coil after the RF pulse in order not to attenuate the magnetic field of the RF coil. The parameters of the magnetization and detection coil used in our experiments are given in Table 1. The measured S/N ratios for 1 liter water samples and shielding factors for different magnetization coil terminations are given in Table 2. The theoretical shielding factors are given in the same table. The difference between the observed and calculated shielding factors results from the electric field oscillations picked up by the capacitance of the detection coil, by the inhomogeneity of the magnetic-field oscillations, and from the thermal noise background. It is also important to remember that the shielding coil attenuates only the component of the external oscillating magnetic field that is parallel to the coil axis. The perpendicular component is only slightly attenuated, depending on the diameter of the wire. Since the effective cross section of the detection coil with many turns is in general not perpendicular to the coil axis, there is always a component of the external oscillating magnetic field that cannot be shielded in the way described above.

CONCLUSIONS

In weak-field MRI systems that perform field cycling of the static magnetic field by switching the resistive coils, the efficient shielding of the detection coil from low-frequency magnetic interference can be achieved by using the magnetization coil or one of the coils as a shield. The theory and measurements show that significant improvement in shielding the axial component of magnetic interference at

TABLE 2
Shielding Factors and S/N Ratios for Different Magnetization Coil Termination

Termination	U_{RMS} (mV)	F_{meas}	F_{calc} (2 kHz)	S/N
Open	8.45 ± 0.5	1	1	24
Short	1.81 ± 0.1	0.21 ± 0.02	0.09	112
L_{opt}	1.38 ± 0.1	0.16 ± 0.02	0.009	147

Note. S/N values has been calculated measuring the signal amplitude from 1 liter water sample after 90° pulse and RMS values of noise.

the center of the coil can be achieved by adding a suitable series impedance to the shielding coil during signal detection. The optimal impedance is determined by the geometry of the coil and the observed frequency. The optimal impedance is capacitive for short coils or inductive for long coils.

ACKNOWLEDGMENTS

The author thanks Professor Janez Stepišnik for useful discussions and for reviewing the manuscript and Mr. Vital Eržen for technical help.

REFERENCES

1. G. Planinšič, J. Stepišnik, and M. Kos, *J. Magn. Reson. A* **110,** 170 (1994).
2. S. Conolly, T. Brosnan, and A. Macovski, Abstracts of the Society of Magnetic Resonance, 3rd Annual Meeting, Nice, p. 935, 1996.
3. B. Favre, J. P. Bonche, H. Mehier, and J. O. Peyrin, *Magn. Reson. Med.* **15,** 386 (1990).
4. D. J. Lurie, J. M. S. Hutchison, L. H. Bell, I. Nicholson, D. M. Bussell, and J. R. Mallard, *J. Magn. Reson.* **84,** 431 (1989).
5. D. Grucker, *Magn. Reson. Med.* **14,** 140 (1990).
6. J. Stepišnik, V. Eržen, and M. Kos, *Magn. Reson. Med.* **15,** 386 (1990).
7. D. Korbee, T. Classen-Vujčič, H. M. Borsboom, H. Konijnenburg, J. Creyghton, J. Trommel, and A. F. Mehlkopf, Abstracts of the Society of Magnetic Resonance, 3rd Annual meeting, Nice, p. 933, 1996.
8. E. Jahnke and F. Emde, ''Tables of Functions with Formulae and Curves,'' 4th ed., Dover, New York, 1945.